

PHOTONIC CRYSTAL STRUCTURES

PACS numbers: 42.70.Qs; 42.25.Bs; 78.67.Ss
DOI: 10.1070/QE2012v042n06ABEH014822

Defect mode suppression in a photonic crystal structure with a resonance nanocomposite layer

S.G. Moiseev, V.A. Ostatochnikov, D.I. Sementsov

Abstract. **This paper examines the key features of the transmission and reflection spectra of a one-dimensional photonic crystal structure in which a nanocomposite layer is sandwiched between dielectric Bragg mirrors. Two orthogonal polarisations of an incident wave correspond to different plasmon resonance frequencies of the nanocomposite. If one of the plasmon frequencies coincides with the defect mode frequency in one of the photonic bandgaps, complete suppression of the defect mode in the transmission spectrum is possible, which makes the spectra of such structures polarisation-sensitive.**

Keywords: *nanocomposite, photonic crystal, bandgap, defect mode.*

1. Introduction

One-dimensional (1D) photonic crystal structures (PCS's) formed by a periodic arrangement of layers of different materials have recently attracted a great deal of attention. Owing to the periodic modulation of their refractive index, the photon spectrum of such structures has a bandgap, with an almost total reflection of incident light. This property is of importance for various practical applications of PCS's, including control of optical radiation in laser engineering and information transfer systems. Of particular interest in this context is a Fabry–Perot microcavity structure, which has the form of a 'defect' layer sandwiched between two Bragg mirrors (1D photonic crystals). The defect layer in such a PCS acts as an optical microcavity where an optical field can be localised, which considerably enhances many effects pertaining to light–matter interaction [1, 2].

The functionality of PCS's can be extended through control of their spectral characteristics by varying their geometric and physical parameters. In particular, the photon spectrum of a PCS can be significantly modified by disturbing its periodicity [3–5] or by using materials with controllable properties, e.g. nonlinear, resonant or magnetogyrotropic materials [6–11]. Potentially attractive photonic crystal (PC) microcavity materials are metal–dielectric nanocomposites, which have high optical dispersion in the plasmon resonance region [12–16]. D'yachenko and Miklyaev [17] and Vetrov et al. [18] investigated the relationship between the structural parameters of a plasmonic nanocomposite and the spectral properties of the PCS. In this paper, we report the transmission and reflection of a 1D PCS containing a nanocomposite defect layer whose optical characteristics depend on the incident light polarisation.

S.G. Moiseev Kotel'nikov Institute of Radio Engineering and Electronics (Ulyanovsk Branch), Russian Academy of Sciences, ul. Goncharova 48/2, 432011 Ulyanovsk, Russia; Ulyanovsk State University, ul. L. Tolstogo 42, 432700 Ulyanovsk, Russia; e-mail: serg-moiseev@yandex.ru;
V.A. Ostatochnikov, D.I. Sementsov Ulyanovsk State University, ul. L. Tolstogo 42, 432700 Ulyanovsk, Russia; e-mail: ostatochnikov_vladimir@mail.ru, sementsovdi@mail.ru

Received 2 February 2012; revision received 2 April 2012
Kvantovaya Elektronika **42** (6) 557–560 (2012)
Translated by O.M. Tsarev

2. Material parameters of the PCS

Consider a symmetric microcavity PCS in which a nanocomposite layer is sandwiched between two dielectric PC mirrors inverted relative to one another (Fig. 1). The structure has a double defect: inversion and inserted layer. The inversion is due to the change in the stacking sequence of the layers in going from one part of the structure to the other. Each part is a dielectric PC mirror, i.e. a periodic structure. It can be described by the formula $\hat{N} = (\hat{N}_1\hat{N}_2)^a$ or $\overline{\hat{N}} = (\hat{N}_2\hat{N}_1)^a$, where a determines the number of structural periods in the PC mirror. To the inverted period corresponds a transfer matrix whose elements are related to those of the matrix for the normal period by $\overline{N}_{\alpha\beta} = N_{3-\beta 3-\alpha}$, where $\alpha, \beta = 1, 2$ [19]. The PC mirrors have a finite number of structural periods, each consisting of two layers of isotropic dielectrics having permittivity ε_j and thickness L_j ($j = 1, 2$). We neglect absorption in the frequency range of interest, so ε_j is real-valued and both $\hat{N}$ and $\overline{\hat{N}}$ are unimodular matrices with unity determinant. In modelling the optical properties of the structure, we use the following permittivities of the layers in the PC mirrors: $\varepsilon_1 = 5.52$ (TiO_2) and $\varepsilon_2 = 2.25$ (SiO_2) [20].

The defect layer in the PCS consists of a nanocomposite, which has the form of a dielectric material containing evenly distributed metallic nanoparticles in the shape of ellipsoids of revolution. The nanoparticles are aligned with their polar axis parallel to the x axis. The nanocomposite has properties of a

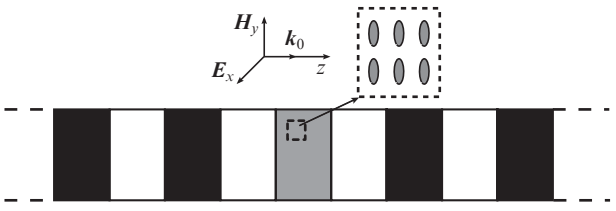

Figure 1. Schematic of the nanocomposite microcavity with dielectric Bragg mirrors.

uniaxial crystal, and its effective permittivity is represented in the major axes by a diagonal tensor with components $\varepsilon_x = \varepsilon_\parallel$ and $\varepsilon_y = \varepsilon_z = \varepsilon_\perp$. (Here and in what follows, the subscripts $\parallel$ and $\perp$ refer to two orientations of the electric field vector of the wave: along and across the optic axis of the nanocomposite.)

In analysis of the optical properties of the PCS, we use the effective medium approximation. Among the diversity of known effective medium models, the nanocomposite under consideration is best represented by the Maxwell Garnett model, in which the effective permittivities have the form [21]

$$\varepsilon_{\perp,\parallel} = \varepsilon_m\left[1 + \frac{\eta(\varepsilon_p - \varepsilon_m)}{\varepsilon_m + (1-\eta)(\varepsilon_p - \varepsilon_m)g_{\perp,\parallel}}\right], \quad (1)$$

where ε_m and ε_p are the permittivities of the matrix and inclusions, respectively; η is the volume fraction of the inclusions; and $g_{\perp,\parallel}$ are geometric factors that take into account the effect of nanoparticle shape on the induced dipole moment of the nanoparticles. Neglecting the absorption and frequency dispersion in the dielectric matrix, we take ε_m to be constant and real-valued. The permittivity of the metallic nanoparticles is given by

$$\varepsilon_p(\omega) = \varepsilon_0 - \frac{\omega_p^2}{\omega^2 + i\omega\gamma}, \quad (2)$$

where ω_p is the plasmon frequency; ε_0 is the lattice contribution; and γ is the relaxation parameter. The geometric factor can be expressed through the ratio of the semi-polar axis to the semi-equatorial axis of the nanoparticles:

$$g_\parallel = \frac{1}{1-\xi^2}\left(1 - \xi\frac{\arcsin\sqrt{1-\xi^2}}{\sqrt{1-\xi^2}}\right), \quad g_\perp = (1 - g_\parallel)/2. \quad (3)$$

The magnetic permeabilities of all the layers in the structure are taken to be unity.

In the numerical analysis below, the nanoparticle material is silver for definiteness: $\omega_p = 1.36\times10^{16}$ s^{-1}, $\varepsilon_0 = 5$, $\gamma = 3.04\times10^{13}$ s^{-1} [22]. The other parameters are $\eta = 10^{-3}$, $\xi = 0.55$ and $\varepsilon_m = 2.25$ (SiO_2). These parameters correspond to the nanocomposite described by Wang et al. [23]. In the fabrication of such nanocomposites, wide use is made of a low-temperature process in which a softened (~600 °C) mixture of glass and silver nanoparticles is rolled out, drawn or extruded under pressure to give films containing nanoparticles of desired shape and orientation. In the nanocomposites thus produced, the inclusions have a high degree of orientation ordering and are evenly distributed over the matrix [23–27].

Figure 2 shows the frequency dependences of the real and imaginary parts of the effective permittivities of the nanocomposite. The permittivities are seen to exhibit resonant behaviour, with different resonance frequencies of $\varepsilon_\perp$ and $\varepsilon_\parallel$ ($\omega_\perp = 3.99\times10^{15}$ s^{-1}, $\omega_\parallel = 5.07\times10^{15}$ s^{-1}), which eventually leads to a significant dependence of the optical properties of the nanocomposite on the polarisation of propagating waves. The observed resonances are associated with the plasmon resonances of the nanoparticles, and their frequencies depend on the orientation of the optic axis of the nanoparticles with respect to the light vector of the electromagnetic wave [15, 28, 29].

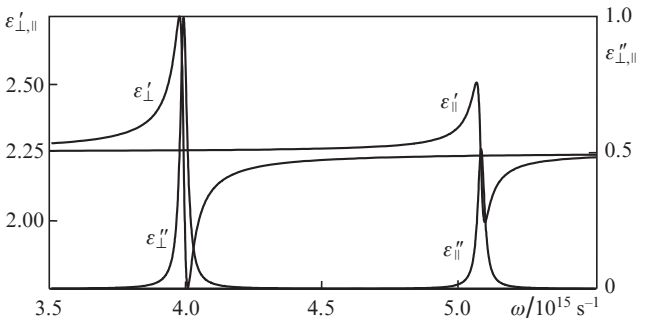

Figure 2. Frequency dependences of the real ($\varepsilon'_{\perp,\parallel}$) and imaginary ($\varepsilon''_{\perp,\parallel}$) parts of the effective permittivity of the silver-containing nanocomposite at $\xi = 0.55$, $\eta = 10^{-3}$, $\varepsilon_0 = 5$, $\gamma = 3.04\times10^{13}$ s^{-1}, $\omega_p = 1.36\times10^{16}$ s^{-1}.

3. Transfer matrices

Let the z axis be normal to the interfaces between the layers. A wave propagates along this axis, and the PCS is in vacuum. Solving Maxwell's equations, we obtain two orthogonally polarised eigenwaves with electromagnetic field components $(E_x, H_y, 0)$ and $(H_x, E_y, 0)$. In the case of a periodic layered structure, it is convenient to introduce a two-component vector $\boldsymbol{F}$ with components E_x and H_y (for the former type of wave) and a transfer matrix of the entire structure, $\hat{G}$, which links the amplitudes of the incident and transmitted waves: $\boldsymbol{F}_t = \hat{G}\boldsymbol{F}_0$. The transfer matrix of the PCS under consideration, with an inserted defect layer and two PC mirrors, has the form $\hat{G} = \hat{N}^a\hat{D}\hat{\bar{N}}^b$, where $\hat{N}^a = (\hat{N}_1\hat{N}_2)^a$ and $\hat{\bar{N}}^b = (\hat{N}_2\hat{N}_1)^b$ are the transfer matrices of defect-free PC mirrors having a and b periods, respectively [19]. The right-hand PC mirror is an inverted structure because it has an inverted sequence of layers. The transfer matrix of the defect layer has the form

$$\hat{D} = \begin{pmatrix} \cos(k_d L_d) & i\sqrt{\varepsilon_d}\sin(k_d L_d) \\ -(i/\sqrt{\varepsilon_d})\sin(k_d L_d) & \cos(k_d L_d) \end{pmatrix}, \quad (4)$$

where L_d is the thickness of the defect layer; $k_d = k_0\sqrt{\varepsilon_d}$; and $\varepsilon_d = \varepsilon_\parallel$ or $\varepsilon_\perp$, depending on the type (polarisation) of the wave propagating through the structure.

The amplitude reflection and transmission coefficients of the PCS in vacuum can be expressed through the elements of the $\hat{G}$ matrix:

$$r = \frac{G_{11} + G_{12} - G_{21} - G_{22}}{G_{11} + G_{12} + G_{21} + G_{22}}, \quad t = \frac{2}{G_{11} + G_{12} + G_{21} + G_{22}}. \quad (5)$$

The reflectance and transmittance are $R = |r|^2$ and $T = |t|^2$.

4. Numerical analysis

Consider the optical characteristics of the PCS. Let the layers in the PC mirrors have identical optical thicknesses, i.e. $L_1\sqrt{\varepsilon_1} = L_2\sqrt{\varepsilon_2} = L_0$, and the optical thickness of the nanocomposite layer is $2L_0$. At these thicknesses, the spectral line of the defect mode lies in the centre of the bandgap of a defect-free PCS. Figure 3 shows the transmission and reflection spectra of an $(\hat{N}_1\hat{N}_2)^6\hat{D}(\hat{N}_2\hat{N}_1)^6$ PCS with a nonresonant defect layer having a real-valued permittivity $\varepsilon_d = \varepsilon_m = 2.25$ and with a resonant defect layer having the same parameters as in the caption to Fig. 2. The spectra are for the first photonic bandgap with a centre frequency $\omega_\perp = 3.99\times10^{15}$ s^{-1},

corresponding to a structure with $\varepsilon_d = \varepsilon_\perp$ and layer thicknesses $L_1 = 79$ nm, $L_2 = 50$ nm and $L_d = 157$ nm (optical thicknesses $L_1\sqrt{\varepsilon_1} = L_2\sqrt{\varepsilon_2} = L_d\sqrt{\varepsilon_m}/2 = 118$ nm). The double defect – inversion plus insertion – disturbs the periodicity of the PCS and produces narrow transmission bands – so-called defect modes – in the centre of the photonic bandgaps [19]. The reflectance of the nonresonant structure, which is thought to be nonabsorbing, is $R = 1 - T$. The transmittance for the defect mode at frequency $\omega = \omega_\perp$ then has the highest possible value $T = 1$. The resonant structure has near-zero transmission at this frequency for a wave with the corresponding polarisation, i.e. with components H_x, E_y and 0, and two symmetrically arranged peaks, corresponding to low transmission of the structure. The $T(\omega)$ and $R(\omega)$ spectra for a wave with the orthogonal polarisation (E_x, H_y, 0) are almost identical to those of the structure with a nonresonant defect. At frequency $\omega_\perp$, the transmittance for a wave with this polarisation differs little from unity. The reason for this is that, in the frequency range in question, $\varepsilon_\parallel = \varepsilon_m$ with high accuracy.

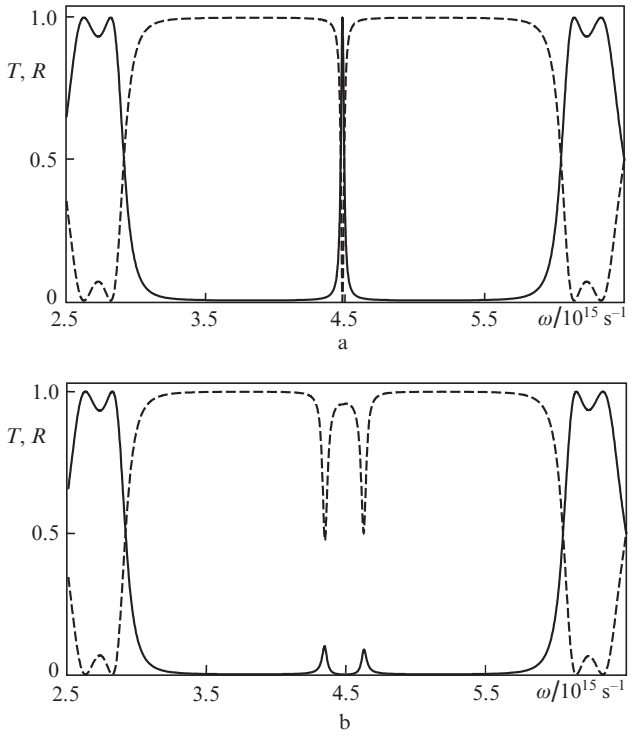

Figure 3. Transmission and reflection spectra (solid and dashed lines, respectively) of an $(\hat{N}_1\hat{N}_2)^6\hat{D}(\hat{N}_2\hat{N}_1)^6$ PCS with (a) a nonresonant ($\varepsilon_d = \varepsilon_m$) and (b) a resonant [$\varepsilon_d = \varepsilon_\perp(\omega)$] defect layer.

For a wave with field components E_x, H_y and 0, the transmission and reflection spectra corresponding to the first photonic bandgap of an $(\hat{N}_1\hat{N}_2)^6\hat{D}(\hat{N}_2\hat{N}_1)^6$ structure are presented in Fig. 4. The spectra are similar to those in Fig. 3. In this case, however, $\varepsilon_d = \varepsilon_\parallel$, and, for the resonance frequency, $\omega_\parallel = 5.070\times10^{15}$ s^{-1}, to equal the centre frequency of the photonic bandgap, the optical thicknesses of the layers should be $L_1\sqrt{\varepsilon_1} = L_2\sqrt{\varepsilon_2} = L_d\sqrt{\varepsilon_m}/2 = 93$ nm (the actual thicknesses are $L_1 = 62$ nm, $L_2 = 40$ nm and $L_d = 124$ nm). The structure also has near-zero transmission at the centre frequency for the type of wave under consideration and almost complete transmission for a wave with the orthogonal polarisation. Thus,

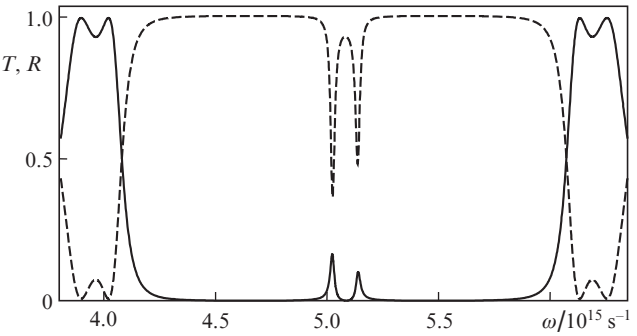

Figure 4. Transmission and reflection spectra (solid and dashed lines, respectively) of an $(\hat{N}_1\hat{N}_2)^6\hat{D}(\hat{N}_2\hat{N}_1)^6$ PCS at $\varepsilon_d = \varepsilon_\parallel(\omega)$.

the insertion of a nanocomposite defect layer into a PCS makes its transmission and reflection spectra polarisation-sensitive.

In addition, the parameters of the nanocomposite and the PCS as a whole can be adjusted so that the resonance frequencies $\omega_\perp$ and $\omega_\parallel$ will be equal to the centre frequencies of the neighbouring photonic bandgaps ($\omega_\perp = 3.967\times10^{15}$ s^{-1} and $\omega_\parallel = 5.100\times10^{15}$ s^{-1}). Figure 5 shows the transmission and reflection spectra of the PCS when the electric field vector of a light wave is oriented across and along the optic axis of the nanocomposite. The material parameters of the structure are the same as in the caption to Fig. 2, and the actual thicknesses of the layers are $L_1 = 554$ nm, $L_2 = 354$ nm and $L_d = 1108$ nm (optical thicknesses $L_1\sqrt{\varepsilon_1} = L_2\sqrt{\varepsilon_2} = L_d\sqrt{\varepsilon_m}/2 = 833$ nm). It is seen that, for both polarisations, one of the two plasmon resonances of the nanoparticles is excited, which leads to defect mode suppression at the corresponding resonance frequency, i.e. in the corresponding photonic bandgap. At the

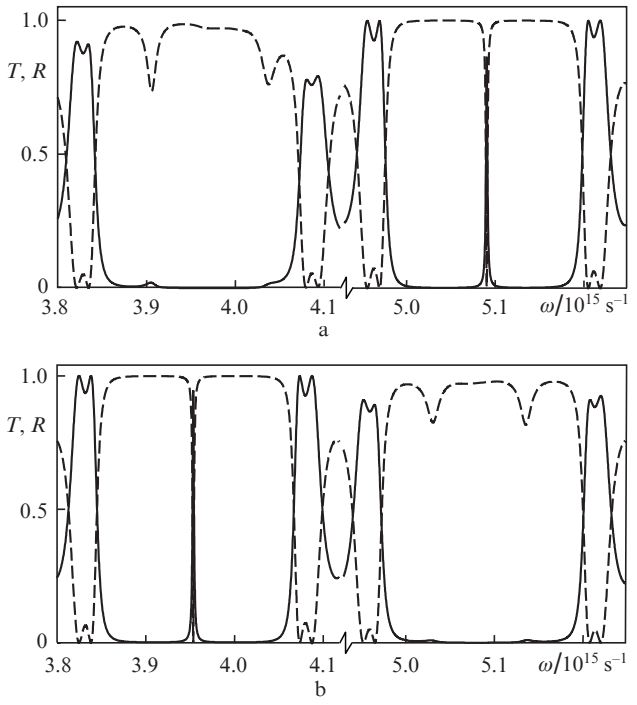

Figure 5. Transmission and reflection spectra (solid and dashed lines, respectively) of an $(\hat{N}_1\hat{N}_2)^6\hat{D}(\hat{N}_2\hat{N}_1)^6$ PCS at (a) $\varepsilon_d = \varepsilon_\perp$ and (b) $\varepsilon_d = \varepsilon_\parallel(\omega)$.

layer thicknesses chosen above, the numbers of the neighbouring photonic bands are seven and nine because, when the layers in a PCS have identical optical thicknesses, its transmission and reflection spectra have only odd photonic bandgaps [19]. As seen from the above data, orthogonal polarisations of waves correspond to defect mode suppression in different photonic bandgaps. This property of the PCS considered here can be used to control laser light polarisation.

Acknowledgements. This work was supported by the Russian Foundation for Basic Research and the RF Ministry of Education and Science (federal targeted programme Scientists and Teachers of Innovative Russia, 2009–2013).

References

1. Inoue K., Ohtaka K. *Photonic Crystals: Physics, Fabrication and Applications* (Berlin: Springer, 2004).
2. Mantsyzov B.I. *Kogerentnaya i nelineinaya optika fotonnykh kristallov* (Coherent and Nonlinear Optics of Photonic Crystals) (Moscow: Fizmatlit, 2009).
3. Zheltikov A.M., Magnitskii S.A., Tarasishin A.V. *Zh. Eksp. Teor. Fiz*., **117**, 691 (2000) [*JETP*, **90**, 600 (2000)].
4. Zabolotin A.E. et al. *J. Opt. Soc. Am. B*, **28**, 2216 (2011).
5. Vetrov S.Ya., Shabanov A.V. *Zh. Eksp. Teor. Fiz*., **120**, 1126 (2001) [*JETP*, **93**, 977 (2001)].
6. Andreani L.C., Cattaneo F., Guizzetti G., et al. *Phys. E*, **17**, 402 (2003).
7. Arkhipkin V.G., Myslivets S.A. *Kvantovaya Elektron*., **39**, 157 (2009) [*Quantum Electron*., **39**, 157 (2009)].
8. Vetrov S.Ya., Timofeev I.V., Avdeeva A.Yu. *Opt. Spektrosk*., **109**, 111 (2010) [*Opt. Spectrosc*., **109**, 106 (2010)].
9. Erokhin S.G., Vinogradov A.P., Granovskii A.B., Inoue M. *Fiz. Tverd. Tela*, **49**, 477 (2007) [*Phys. Solid State*, **49**, 497 (2007)].
10. Hamidi S.M., Tehranchi M.M. *J. Lightwave Technol*., **28**, 2139 (2010).
11. Eliseeva S.V., Sementsov D.I. *Zh. Eksp. Teor. Fiz*., **139**, 235 (2011) [*JETP*, **112**, 199 (2011)].
12. Oraevskii A.N., Protsenko I.E. *Kvantovaya Elektron*., **31**, 252 (2001) [*Quantum Electron*., **31**, 252 (2001)].
13. Sukhov S.V. *Kvantovaya Elektron*., **35**, 741 (2005) [*Quantum Electron*., **35**, 741 (2005)].
14. Moiseev S.G. *Izv. Vyssh. Uchebn. Zaved., Ser. Fiz*., **52** (11), 7 (2009) [*Russ. Phys. J*., **52** (11), 1121 (2009)].
15. Moiseev S.G. *Appl. Phys. A*, **103**, 775 (2011).
16. Moiseev S.G. *Appl. Phys.* A, **103**, 619 (2011).
17. D'yachenko P.N., Miklyaev Yu.V. *Komp'yut. Opt*., **31**, 31 (2007).
18. Vetrov S.Ya., Avdeeva A.Yu., Timofeev I.V. *Zh. Eksp. Teor. Fiz.*, **140**, 871 (2011) [*JETP*, **113**, 755 (2011)].
19. Eliseeva S.V., Sementsov D.I. *Opt. Spektrosk*., **109**, 790 (2010) [*Opt. Spectrosc*., **109**, 729 (2011)].
20. Tsurumachi N., Yamashita S., Muroi N., Fuji T., Hattori T., Nakatsuka H. *Jpn. J. Appl. Phys*., **11**, 38 (1999).
21. Bohren C.F., Huffman, D.R. *Absorption and Scattering of Light by Small Particles* (New York: Wiley, 1983; Moscow: Mir, 1986).
22. Johnson P.B., Christy R.W. *Phys. Rev. B*, **6**, 4370 (1972).
23. Wang D., Guo S., Yin S. *Opt. Eng*., **42**, 3585 (2003).
24. Stookey S.D., Araujo R. *J. Appl. Opt*., **7**, 777 (1968).
25. Lentz W.P., Seward III T.P., Shay G.C. U.S. Patent No. 4,486,213 (1984).
26. Kuang-Hsin K.L., Nolan D.A. U.S. Patent No. 4,282,022 (1981).
27. Borek R., Berg K.-J., Berg G. *Glastech. Ber*., **71**, 352 (1998).
28. Klimov V.V. *Nanoplasmonics* (Singapore: Pan Stanford, 2010; Moscow: Fizmatlit, 2010).
29. Moiseev S.G. *Opt. Spektrosk*., **111**, 264 (2011) [*Opt. Spectrosc*., **111**, 233 (2011)].